Dynamic Analysis of Tunnels in Western Ghats of Indian Peninsula: Effect of Shape and Weathering

Mohammad Zaid and M. Rehan Sadique

Abstract The rapid urbanization in the twentieth century has increased the demand of a smart transportation system for the movement of goods and services. The geotechnical structures required the proper study, analysis and application of theoretical, analytical and numerical model(s) from the stability, safety and sustainability aspect. In the present research work, the stability analysis of different tunnel shapes for four different earthquake zones using the finite element analysis has been carried out. The Mohr–Coulomb material constitutive model has been implemented for the elasto-plastic behaviour of the basalt rock mass using 2D plane strain modelling. Three different shapes of tunnel, circular, horseshoe and arch, under four earthquakes of different magnitudes have been considered (i.e. 4.6, 5.6, 6.5 and 7.4 M). The present study suggested that arch-shaped tunnel is stable in all earthquake zones while the horseshoe-shaped tunnel is the most unstable. The effect of depth of overburden has been also considered for each case by varying the overburden depth in three intervals (5, 10 and 17.5 m). The study further reveals that with the increase in depth of overburden, the stability of the tunnel increases. It is also suggested that the weathering of rock has a significant effect on the deformations in tunnels which may in turn increase the instability of tunnel.

Keywords Basalt · Tunnel · Rock · Mohr–Coulomb · Earthquake

1 Introduction

Improvement of transportation infrastructure in urban areas for the transport of goods and mass rapid transit has increased the research interest in the study of tunnels [1–3]. Amorosi and Boldini carried out the study of the dynamic behaviour of the circular tunnel in clayey soil using the finite element method [4]. The authors further concluded that a seismic event can produce a substantial modification of loads acting

M. Zaid (✉) · M. Rehan Sadique
Department of Civil Engineering, ZHCET, Aligarh Muslim University, Aligarh, UP, India
e-mail: mohammadzaid1@zhcet.ac.in

K. K. Pathak et al. (eds.), *Recent Trends in Civil Engineering*, Lecture Notes in Civil Engineering 77, https://doi.org/10.1007/978-981-15-5195-6_57

in the lining. Yu et al. studied the longitudinal seismic response of tunnel liner using an analytical approach [5].

The shape of the tunnel plays a pivotal role when deformation study is carried out. Several researchers have studied the effect of tunnel shape on the stability of the tunnel [6–11]. Augarde and Burd described the finite element for the deformations in case of the shallow tunnel and concluded that a thin layer of the continuum may be used for modelling a tunnel lining for soil–structure interaction problems [12]. Chungsik Yoo studied the longitudinal reinforced face of the tunnel using finite element analysis and concluded that the face deformations can be reduced by the application of longitudinal pipes as face reinforcement [13].

Nevertheless, authors have not found any open literature dealing with the effect of weathering of a rock mass on the behaviour of the tunnel. In the present study, weathering effect of rock, the mass has been incorporated with different opening shapes, different magnitude seismic loadings and varying depth of tunnels. The present paper provides a comparative study by considering four different stages of weathering for three different shapes of tunnels, i.e. circular-shaped tunnel, arch-shaped tunnel and horseshoe-shaped tunnel. These cases have been analysed under four different magnitude earthquake loadings. The effect of depth of overburden has also been considered for each case by varying the overburden depth in three intervals, i.e. 5, 10 and 17.5 m.

2 Numerical Model

The dynamic analysis has been carried out for the 2D plane strain model of 42 m $\times$ 42 m size using finite element software Abaqus/Dynamic. Arch-shaped, circular-shaped and horseshoe-shaped tunnels are drawn having a 7 m diameter, and thickness of tunnel lining has been taken as 120 mm. The three depths of overburden, 5, 10, and 17.5 m, are considered to compare the effect of overburden depth under different (4.6, 5.6, 6.5 and 7.4 M) magnitudes of earthquakes for different stages of rock mass weathering (fresh basalt, slightly weathered, medium weathered and highly weathered basalt). The CPE3R-three-noded plane strain linear triangular element with reduced integration and hourglass control element type has been used for meshing the model. 500 m of overburden due to the already present rock mass has been taken into account in the form of pressure at the top line of the model. The infinite boundary condition has been adopted at the side faces of the tunnel model [14]. The CINPE4, a four-noded linear infinite quadrilateral element, was used for the infinite boundary condition meshing. 1.5 m mesh size has been used for meshing the rock mass and 0.1 m for meshing the tunnel lining (Fig. 1).

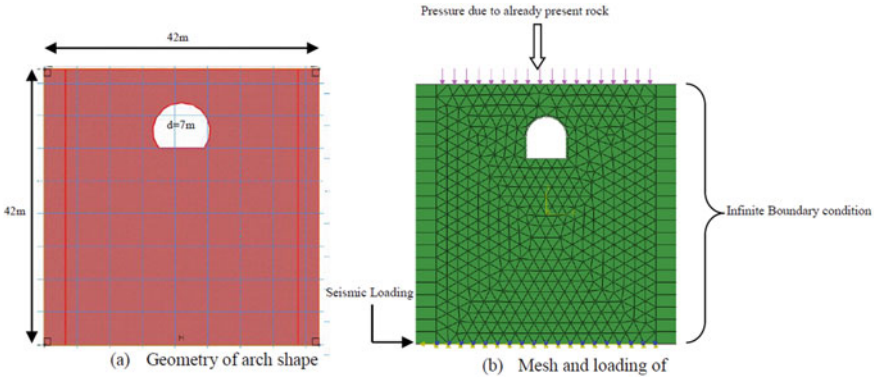

Fig. 1 The geometry of tunnel and meshed model

3 Input Properties

The Mohr–Coulomb model of elasto-plastic material has been considered for the behaviour of the rockmass. Various properties of different rockmass taken in the present study are shown in Table 1 [15–21]. The different weathering stages considered in the present study are fresh basalt (W_0), slightly weathered basalt (W_1), medium weathered basalt (W_2) and highly weathered basalt (W_3).

3.1 Analysis

The model was prepared using Abaqus/CAE and boundary conditions were applied. The vertical sides of the model were restrained in position by creating infinite boundary conditions. The earthquake loading has been applied at the base of the model in the form of the acceleration-time history of different earthquakes. The acceleration versus time history plot is shown in Fig. 2.

Table 1 Properties of different weathering stages [22]

Rockmass	Modulus of elasticity (GPa)	Poisson's ratio (ν)	Density (kg/m^3)	Friction angle (°)	Dilation angle (°)	Cohesion (MPa)
Basalt (W_0)	46.50	0.186	2960	63.38	12	26.25
Basalt (W_1)	20.60	0.260	2740	53.71	12	18.50
Basalt (W_2)	02.80	0.272	2470	33.33	04	08.08
Basalt (W_3)	00.60	0.272	1820	43.87	00	01.64
Concrete	31.6	0.15	2400			

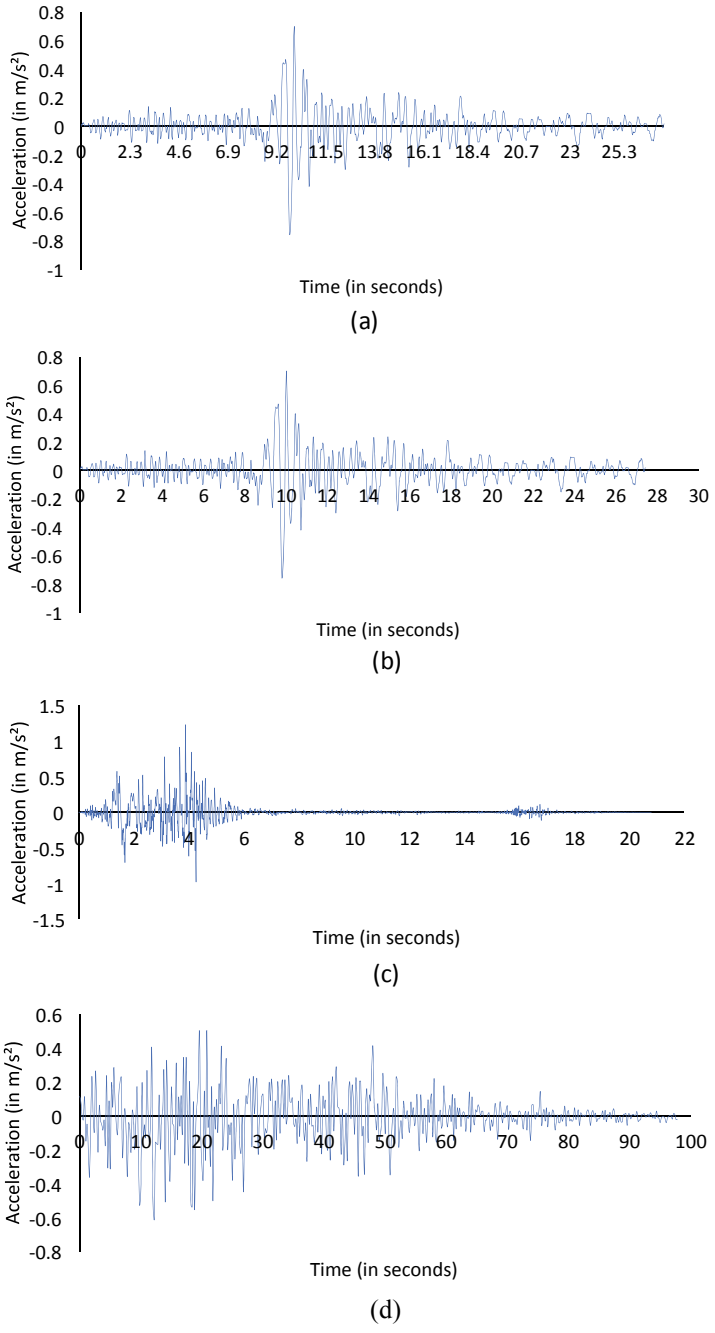

Fig. 2 Acceleration-time history of **a** 4.6 M, **b** 5.6 M, **c** 6.5 M and **d** 7.4 M magnitude of earthquake [23]

4 Results and Discussion

In the present paper, different shapes of the tunnel are analysed under different earthquake conditions. The weathering of the basalt rock has also been considered. The four weathering stages of basalt rock adopted in the present paper are; fresh basalt (W_0), slightly weathered basalt (W_1), medium weathered basalt (W_2) and highly weathered basalt (W_3). The depth variation has also been taken into account. There are three depths of overburden 5, 10 and 17.5 m adopted in the present analysis. The finite element software Abaqus/Explicit has been adopted for the present study. The paper focuses on the comparison of the stability of different shapes in different magnitudes of earthquakes.

The comparison of the depth of overburden has been shown in Table 2. It can be seen from the table that with the increase in the depth of overburden the deformation decreases. For the 4.6 M magnitude of the earthquake, a 5% decrease in deformation has been observed for the increase in depth of overburden from 5 m to 10 m.

For an increase in depth of overburden from 10 to 17.5 m, a 3.5% decrease in deformation has been observed. Similarly, for the 5.6 M magnitude of the earthquake, an increase in depth of overburden from 5 to 10 m and 10 to 17.5 m shows 12 and 1% decrease in the values of deformations, respectively. And for the 6.5 M magnitude of the earthquake, 16 and 3% decrease in the value of deformation has been observed for the similar increase in depth of overburden. Lastly, for 7.4 M magnitude, 28 and 8% decrease in the value of deformation has been observed for the increase in the depth of overburden from 5 m to 10 m and 10 m to 17.5 m, respectively.

The deformation has been plotted against each weathering stage for comparing the depth of overburden in Fig. 3 for the arch-shaped tunnel. This shows that weathering has a significant effect on deformation. Also, as the depth of overburden increases the deformation of the tunnel decreases. Figure 3 shows the results for 4.6 M of earthquake for different shapes of the tunnel.

The graph shows that as the weathering stage of a basalt rock increases, it results in an increase in deformation at each depth of overburden. Also, as the depth of overburden increases, the deformation reduces as the situation results to lead towards the lithostatic condition.

Table 3 shows the comparison of different shapes of tunnels considered in the present study. It is noted that in the case of fresh basalt (W_0), an arch-shaped tunnel is the safest and the horseshoe-shaped tunnel is most unstable. Similar is the case with slightly weathered basalt (W_1). But, as the weathering of rock increases, a circular-shaped tunnel becomes the safest and the arch-shaped tunnel is the most unstable tunnel.

Table 2 Deformation for arch-shaped tunnel for medium weathered (W_2) basalt rock at right springer of tunnel

Magnitude of an earthquake	4.6 M			5.6 M			6.5 M			7.4 M		
Depth of overburden	17.5 m	10 m	5 m	17.5 m	10 m	5 m	17.5 m	10 m	5 m	17.5 m	10 m	5 m
Deformation	0.057 m	0.059 m	0.062 m	0.216 m	0.228 m	0.257 m	0.3 m	0.335 m	0.389 m	0.861 m	0.934 m	1.196 m

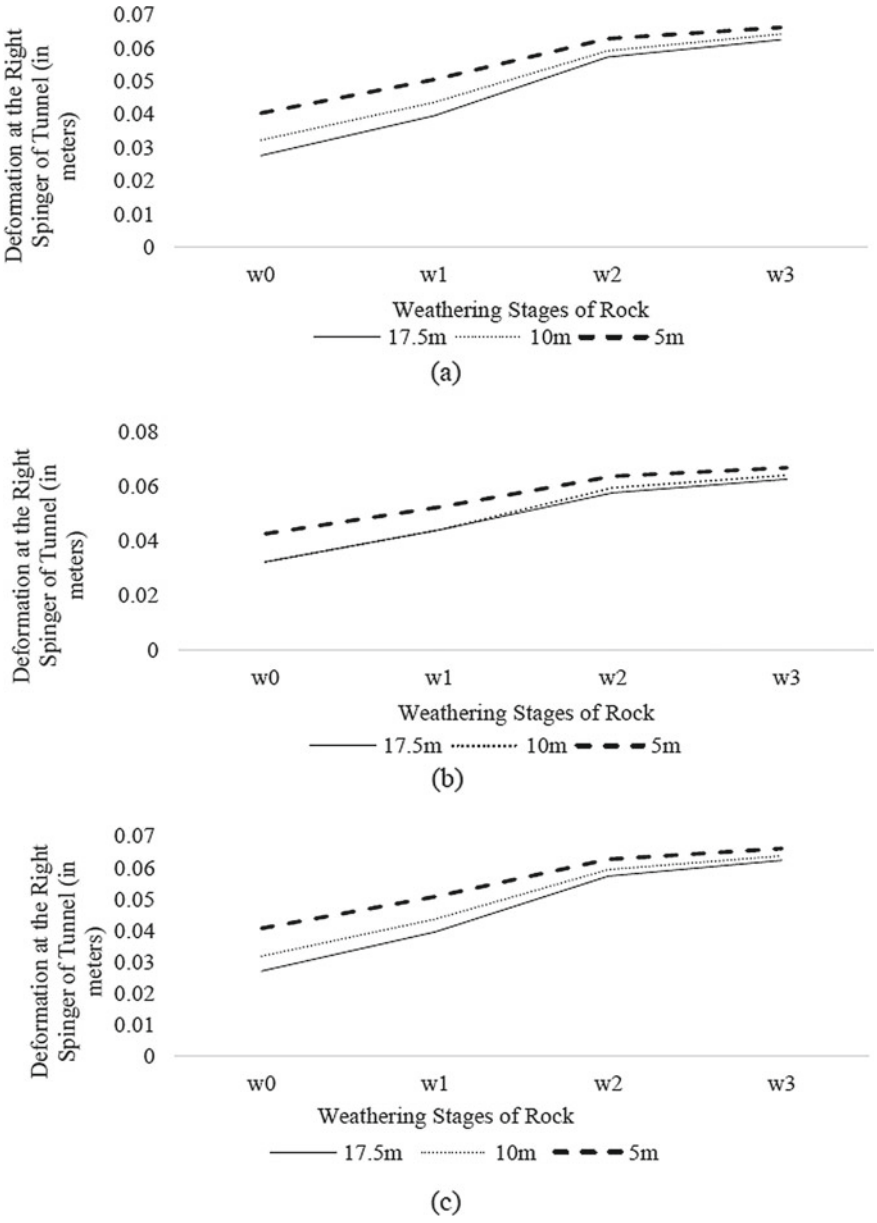

Fig. 3 Comparison of depths for different stages of weathering for **a** arch-shaped tunnel, **b** circular-shaped tunnel and **c** horseshoe tunnel under 4.6 M earthquake loading

Table 3 Comparison of tunnel shape for the 5 m depth of overburden under 7.4 M earthquake loading for different stages of weathering

Weathering stages of rock	W_0			W_1			W_2			W_3		
Shape of tunnel	Circular	Arch	Horseshoe	Circular	Arch	Horseshoe	Circular	Arch	Horseshoe	Circular	Arch	Horseshoe
Deformation	0.173 m	0.264 m	0.308 m	0.206 m	0.353 m	0.363 m	0.646 m	1.196 m	0.780 m	0.921 m	1.339 m	1.335 m

The magnitude of an earthquake similar to or equal to the 7.4 M makes the comparison clearer, as shown in Fig. 4. In this case, the arch-shaped tunnel is most stable at every depth of overburden. The horseshoe-shaped tunnel has maximum deformation, and thus it is the most unstable shape of a tunnel.

Figure 5 shows a graph for the comparison of the magnitude of an earthquake for the horseshoe shape of the earthquake at 5, 10 and 17.5 m of overburden depth. The magnitude of the 4.6 M earthquake has the least deformation and the 7.4 M magnitude of earthquake has maximum deformation. Figure 5 has been plotted for horseshoe-shaped tunnel, irrespective of shape; the deformation pattern is similar for all shapes of tunnels.

Table 4 shows the comparison between different magnitudes of earthquakes for the deformation readings taken at the right springer of the tunnel. For fresh basalt rock (W_0), it can be noted that an increase of the magnitude of the earthquake from 4.6 to 5.6 M increases the deformation by 27, 33% for an increase in magnitude from 5.6 to 6.5 M and 7.4% increase for 6.5 to 7.4 M increase in the magnitude of the earthquake.

5 Conclusion

A two-dimensional finite element analysis has been performed to study the behaviour of rock tunnels considering weathering effects. Few important observations may be concluded as follows:

- As the weathering stage of a basalt rock increases, due to a loss in structural strength, it results in an increase of deformation in the rock tunnel at each depth of overburden.
- As the depth of overburden increases, the deformation in the rock tunnel reduces. It is may be due to the development of a lithostatic condition.
- In the case of fresh basalt (W_0), arch-shaped tunnel is the safest and the horseshoe-shaped tunnel is most unstable, similarly for slightly weathered basalt (W_1).
- As the weathering of rock increases, circular-shaped tunnel becomes the safest and the arch-shaped tunnel is the most unstable tunnel.
- In case of an earthquake of a magnitude of 7.4 M, the arch-shaped tunnels are most stable at every depth of overburden and the horseshoe-shaped tunnels have maximum deformation, and thus it is the most unstable shape of a tunnel.
- Deformation increases with an increase in the magnitude of the earthquake.

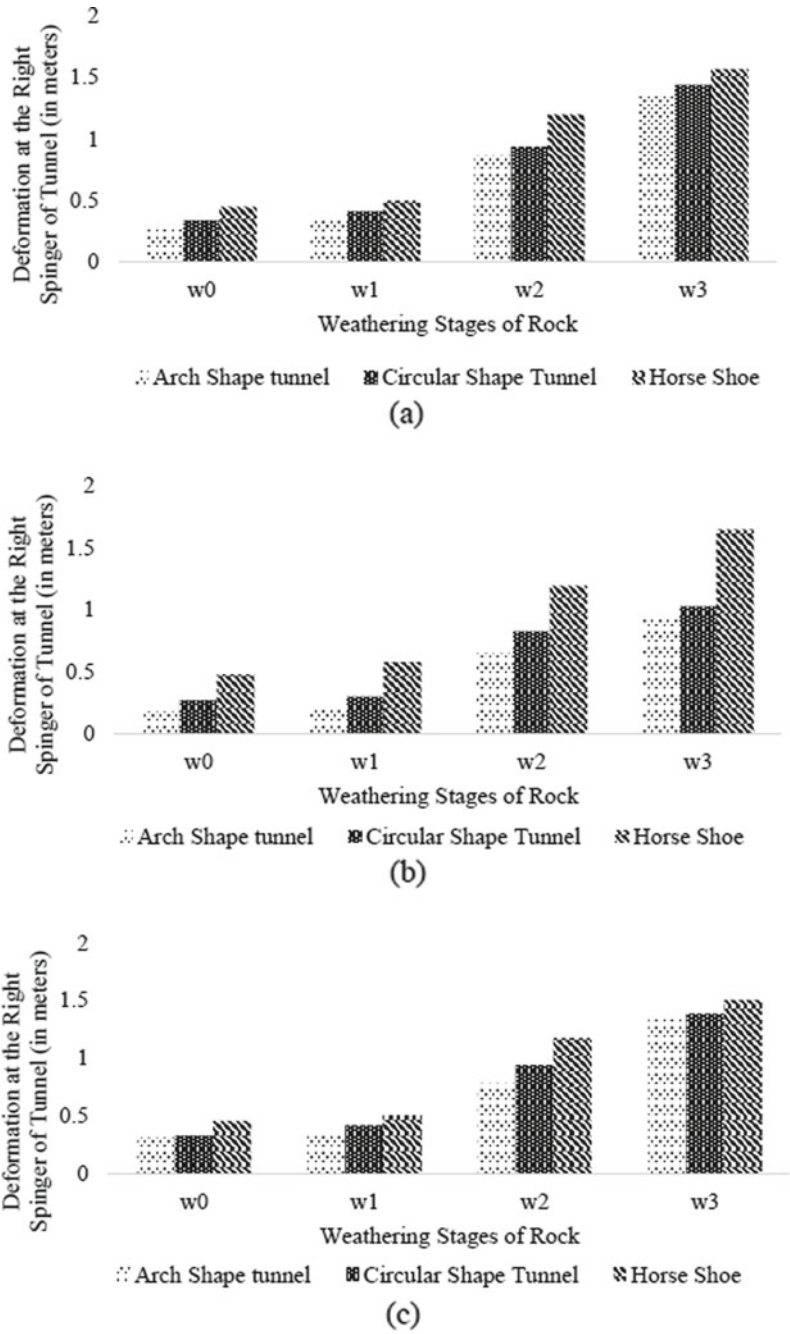

Fig. 4 Comparison of shapes of the tunnel in different stages of weathering for **a** 5 m, **b** 10 m and **c** 17.5 m under 7.4 M earthquake loading

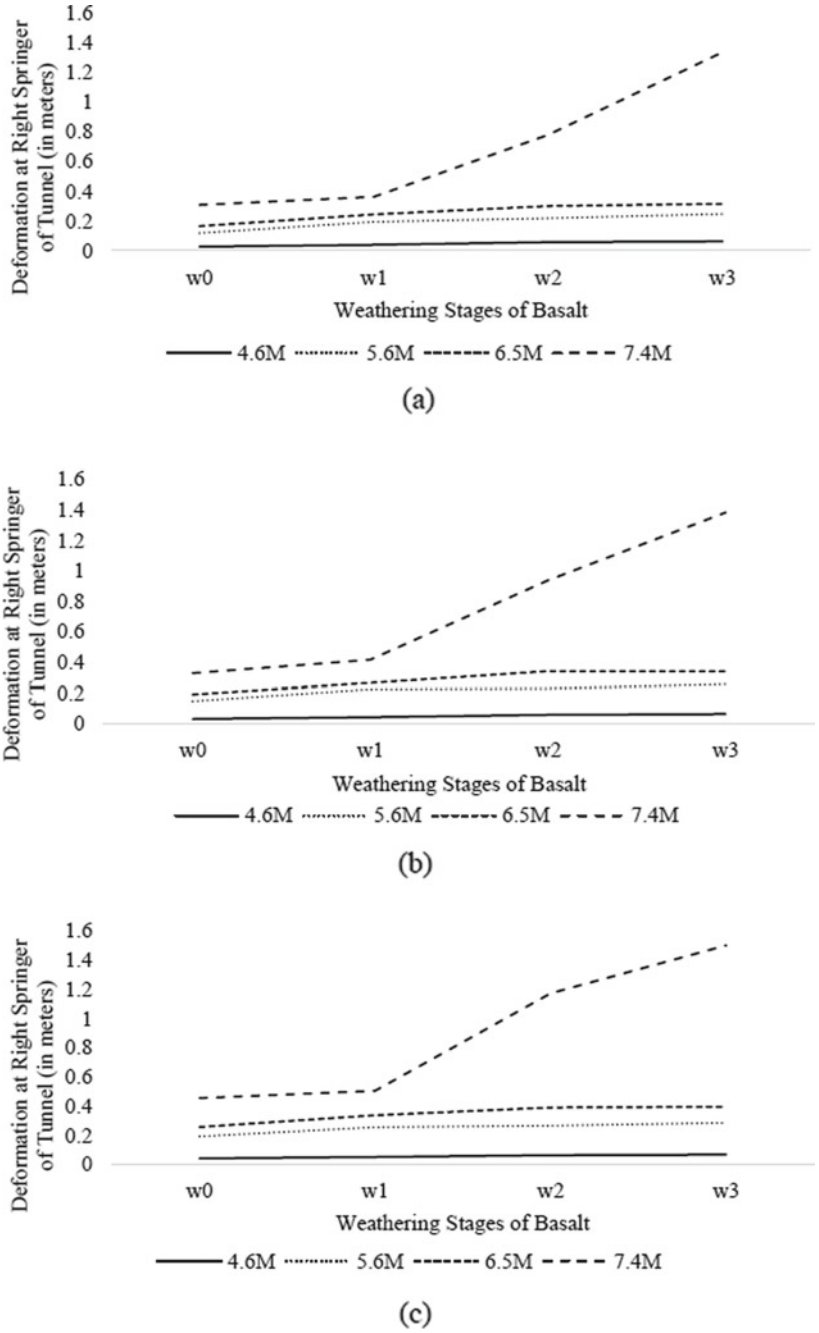

Fig. 5 Comparison of deformation under the different magnitudes of the earthquake in different stages of weathering for **a** 5 m, **b** 10 m and **c** 17.5 m of depth for the horseshoe-shaped tunnel

Table 4 Deformation comparison under the different magnitudes of earthquakes for circular-shaped tunnel at a 5 m depth of overburden (in metres)

Weathering stages	W_0				W_1				W_2				W_3			
Magnitude of an earthquake	4.6 M	5.6 M	6.5 M	7.4 M	4.6 M	5.6 M	6.5 M	7.4 M	4.6 M	5.6 M	6.5 M	7.4 M	4.6 M	5.6 M	6.5 M	7.4 M
Deformation at right springer of tunnel (in metres)	0.032	0.121	0.161	0.173	0.044	0.201	0.244	0.206	0.057	0.215	0.302	0.646	0.062	0.241	0.306	0.921

References

1. Mishra S, Rao KS, Gupta NK, Kumar A (2017) Damage to shallow tunnels under static and dynamic loading. Procedia Eng 173:1322–1329
2. Zhang ZX, Liu C, Huang X, Kwok CY, Teng L (2016) Three-dimensional finite-element analysis on ground responses during twin-tunnel construction using the URUP method. Tunn Undergr Sp Technol 58:133–146
3. Kargar AR, Rahmannejad R, Hajabasi MA (2014) A semi-analytical elastic solution for stress field of lined non-circular tunnels at great depth using complex variable method. Int J Solids Struct 51:1475–1482
4. Amorosi A, Boldini D (2009) Numerical modelling of the transverse dynamic behaviour of circular tunnels in clayey soils. Soil Dyn Earthq Eng 29(6):1059–1072
5. Yu H et al (2018) Analytical solution for longitudinal seismic response of tunnel liners with sharp stiffness transition. Tunn Undergr Sp Technol 77:103–114
6. Banerjee SK, Chakraborty D (2018) Stability analysis of a circular tunnel underneath a fully liquefied soil layer. Tun Undergr Sp Technol 78:84–94
7. Ng CWW, Fong KY, Liu HL (2018) The effects of existing horseshoe-shaped tunnel sizes on circular crossing tunnel interactions: three-dimensional numerical analyses. Tunn Undergr Sp Technol 77:68–79
8. Athar MF, Zaid M, Sadique MR (2019) Stability of different shapes of tunnels in weathering stages of basalt. In: Proceedings of national conference on advances in structural technology. CoAST2019, pp 320–327
9. Chen HL, Xia ZC, Zhou JN, Fan HL, Jin FN (2013) Dynamic responses of underground arch structures subjected to conventional blast loads: curvature effects. Arch Civ Mech Eng 13:322–333
10. Dancygier AN, Karinski YS, Chacha A (2016) A model to assess the response of an arched roof of a lined tunnel. Tunn Undergr Sp Technol 56:211–225
11. Lai J, Fan H, Liu B, Liu T (2011) Analysis of seismic response of shallow large section multi-arch tunnel. Adv Control Eng Inf Sci 15:2–6
12. Augarde CER, Burd HJ (2001) Three-dimensional finite element analysis of lined tunnels. Int J Numer Anal Methods Geomech 25:243–262
13. Yoo C (2002) Finite-element analysis of tunnel face reinforced by longitudinal pipes. Comput Geotech 29:73–94
14. Naqvi MW, Zaid M, Sadique R, Alam MM (2017) Dynamic analysis of rock tunnels Considering joint dip angle: a finite element approach. In: 13th international conference on vibration problems
15. Zaid M, Sadique MR (2019) Effect of Joint Orientation and Weathering on Static Stability of Rock Slope Having. In: 7th Indian young geotechnical engineers conference—7IYGEC 2019 15–16 March 2019, NIT Silchar, Assam, India SILCHAR
16. Zaid M, Talib A, Rehan Sadique Md (2018)Stability analysis of rock slope having transmission tower. IJRECE 6
17. Gahoi A, Zaid M, Mishra S, Rao KS (2017) Numerical analysis of the tunnels subjected to impact loading. In: 7th India Rock Conference IndoRock
18. Zaid M, Mishra S, Rao KS (2018) Finite element analysis of static loading on urban tunnels. In: Indian Geotechnical Conference 2018 (IGC-2018)
19. Zaid M, Khan MA, Sadique MR (2019) Dynamic response of weathered jointed rock slope having the transmission tower. Proc Nat Conf Adv Struct Technol 1:414–422
20. Zaid M, Talib A, Sadique MR (2018) Effect of joint orientation on the seismic stability of rock slope with transmission tower. In: Indian Geotechnical Conference 2018 (IGC-2018)

21. Mishra S, Rao S, Gupta NK (2016) Effect of different loading conditions on tunnel lining in soft rocks. In: ISRM International Symposium–EUROCK 2016, 29–31 August, Ürgüp, Turkey
22. Gupta AS, Rao KS (1998) Index properties of weathered rocks: inter-relationships and applicability. Bull Eng Geol Environ 57:161–172
23. Systems, C. of O. for S.-M. O. Strong Motion Virtual Data Center (VDC) (2018) https://strongmotioncenter.org/vdc/scripts/default.plx. Accessed 15th October 2018